Low-Loss Optical Branching Waveguides Consisting of Anisotropic Materials

Shinnosuke Sawa, *Member, IEEE*, Masahiro Geshiro, *Member, IEEE*, and Fumikazu Takeda

Abstract—**Low-loss branching waveguides of the mode-conversion type consisting of anisotropic materials are proposed and their basic wave-guiding characteristics are studied by means of coupled-mode theory. Two mode-conversion sections are introduced on both input and output sides of a conventional symmetric branching waveguide. Each arm of the branching waveguides is assumed to be a single-mode slab waveguide except for the tapered section. A coupled-mode system of equations describing mode-conversion phenomena with respect to the TM mode in the branching waveguides is derived from the field expansion in terms of local normal modes. A Runge–Kutta–Gill method is used to numerically solve the coupled-mode equations. It is found that the branching waveguides proposed here suffer mode-conversion losses to a much lesser extent than conventional branching waveguides.**

I. Introduction

In optical network systems, lightwave modulators and splitters/combiners will play important roles. Branching waveguides consisting of both isotropic and anisotropic materials have been key elements for these guided wave devices [1]–[4]. Their losses must be as low and their sizes as small as possible, and they must also be simple to fabricate. Some attempts have been made to reduce mode-conversion losses in isotropic branching waveguides [5]–[8]. To the authors' knowledge, however, the same subject for anisotropic cases has not been fully discussed yet, in spite of the great significance from the device design viewpoint [9], [10].

In this paper we propose low-loss branching waveguides of the mode-conversion type consisting of anisotropic materials. Each arm, except for the tapered section, is assumed to be a single-mode slab waveguide composed of uniaxial crystalline materials. It is also assumed that the optical axes, in both core and cladding, are parallel to each other and lie in the plane defined by the propagation direction and the normal of the waveguide surface. Two mode-conversion sections are introduced on the input and output sides of the separating section in order to suppress unnecessary mode conversion. Basic wave-guiding properties in the proposed structures are studied by means of coupled-mode theory. We concentrate our discussion on the mode-conversion phenomena among TM modes since it is the TM mode, in this case, that shows interesting behavior which cannot be observed in the isotropic case [11], [12]. A coupled-mode system of equations describing the mode-conversion phenomena is derived from the field expansion in terms of local normal modes [13, pp. 106–111]. Numerical results, obtained by the Runge–Kutta–Gill method, show that the branching waveguides proposed in the present paper incur mode-conversion losses that are much less than those of conventional branching waveguides.

Manuscript received May 3, 1990; revised March 13, 1991.

S. Sawa was with the Department of Electronics, Ehime University, Bunkyo-3, Matsuyama, Ehime 790, Japan. He is now with the College of Engineering, University of Osaka Prefecture, Sakai, Osaka 591, Japan.

M. Geshiro is with the Department of Electronics, Ehime University, Bunkyo-3, Matsuyama, Ehime 790, Japan.

F. Takeda was with the Department of Electronics, Ehime University, Bunkyo-3, Matsuyama, Ehime 790, Japan. He is now with Nankai Broadcasting Company, Dogo-himata 6-24, Matsuyama, Ehime 790, Japan.

IEEE Log Number 9100140.

II. Analytical Method

A conventional symmetric branching waveguide composed of a uniaxial crystalline material is shown together with the Cartesian coordinate system used for the analysis in Fig. 1. The whole structure is made up of two subsections along the z axis: a tapered section succeeding a single slab waveguide and a separating section followed by two parallel slab waveguides with a separation of h. The width of the waveguide is d everywhere except for the tapered section. The slope of both the tapered and the separating section is θ; ϵ_r and ϵ_d are dielectric tensors in the core and the cladding, respectively. The functions $f(z)$ and $h(z)$ describe the geometrical shape of the core boundaries.

There exist two types of local normal modes. One is that supported by a three-layered slab waveguide in the tapered section, and the other is that guided by a five-layered slab waveguide in the separating section. The waveguide structures supporting these local normal modes are shown in Fig. 2. Suppose optical axes, in both core and cladding, lie in the $x-z$ plane and are parallel to each other. In the waveguide coordinate system, the dielectric tensor is expressed as [11]

$$\epsilon_p = \begin{pmatrix} \epsilon_{pxx} & 0 & \epsilon_{pxz} \\ 0 & \epsilon_{pyy} & 0 \\ \epsilon_{pzx} & 0 & \epsilon_{pzz} \end{pmatrix} \tag{1}$$

0018-9480/91/0700-1140$01.00

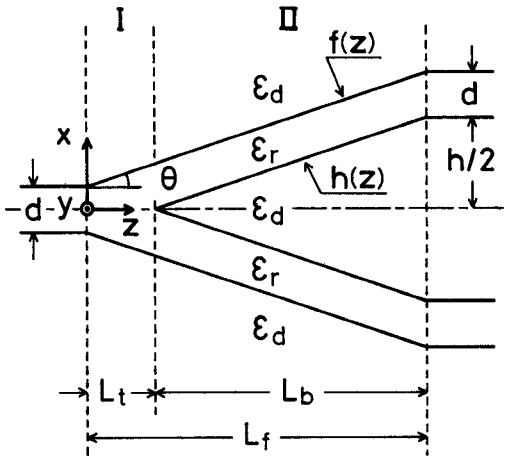

Fig. 1. Conventional branching waveguide.

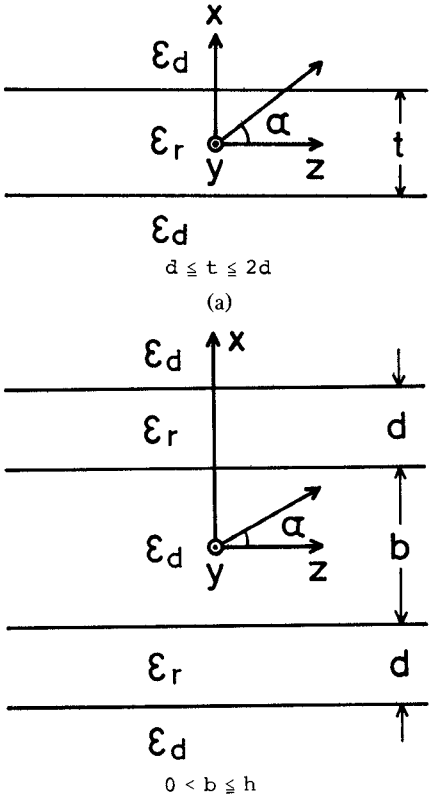

Fig. 2. Waveguides supporting local normal modes: (a) three-layered slab waveguide; (b) five-layered slab waveguide.

where

$$\epsilon_{pxx} = \epsilon_{p1}\cos^2\alpha + \epsilon_{p3}\sin^2\alpha$$
$$\epsilon_{pxz} = \epsilon_{pzx} = (\epsilon_{p3} - \epsilon_{p1})\sin\alpha\cos\alpha$$
$$\epsilon_{pzz} = \epsilon_{p1}\sin^2\alpha + \epsilon_{p3}\cos^2\alpha$$
$$\epsilon_{pyy} = \epsilon_{p1}. \tag{2}$$

In the above equations, ϵ_{p1} and ϵ_{p3} are the principal dielectric constants and α is the angle between the z axis and the optical axis. The subscript p, signifying the region, represents r (core) or d (cladding).

Marcuse [11] tells us that the propagation characteristics of the eigenmodes in the waveguides shown in Fig. 2 do not change significantly through a slight variation in the oblique angle α. For the sake of brevity in the analysis we have chosen these waveguides for the local normal modes. Therefore, the present analysis can be satisfactorily applied to the case where the slopes of the functions $f(z)$ and $h(z)$ are fairly gradual. For a more precise analysis, we should choose a different hypothetical waveguide, one in which the effects of sloping core boundaries could be reflected properly.

We are now treating a weakly guiding structure with a gentle taper and a small separation angle in which coupling between the modes with positive real propagation constants is significant. Thus the coupled-mode equations with respect to the local normal modes can be expressed as [13, pp. 106–111]

$$\frac{da_j(z)}{dz} = \sum_{i(\neq j)} C_{ji}a_i(z)\exp\left[j\int_0^z\{\beta_j(z') - \beta_i(z')\}dz'\right] + \int_0^{\sqrt{\eta_d/\epsilon_0\epsilon_{dxx}}k_0} C_{jr}(z,\rho)a_r(z,\rho) \cdot\exp\left[j\int_0^z\{\beta_j(z') - \beta_r(z',\rho)\}dz'\right]d\rho \tag{3}$$

$$\frac{da_r(z,\rho)}{dz} = \sum_i C_{ri}(z,\rho)a_i(z) \cdot\exp\left[j\int_0^z\{\beta_r(z',\rho) - \beta_i(z')\}dz'\right] \tag{4}$$

where

$$\eta_p = \epsilon_{pxx}\epsilon_{pzz} - \epsilon_{pxz}^2 \tag{5}$$

$$\rho = \sqrt{\frac{\eta_d}{\epsilon_{dxx}^2}\left(\frac{\epsilon_{dxx}}{\epsilon_0}k_0^2 - \beta_r^2\right)}. \tag{6}$$

In the above equations, $a_n(z)$ and $\beta_n(z)$, where $n = i$ or j, are the complex amplitude coefficient and propagation constant of the guided mode labeled n; $a_r(z,\rho)$ and $\beta_r(z,\rho)$ are those of the radiation mode with the transverse propagation constant ρ; and $C_{ji}(z)$, $C_{jr}(z,\rho)$, and $C_{ri}(z,\rho)$ are the coupling coefficients. The parameters ϵ_0 and k_0 are the dielectric constant and the wavenumber in a vacuum, respectively. As mentioned above, (3) and (4) are restricted to coupling between the modes with positive real propagation constants, excluding evanescent modes and backward propagating modes. Coupling between radiation modes is also neglected in the derivation. The coupling coefficient between the modes labeled m and n is given by [13]

$$C_{mn} = \frac{\omega}{4P(\beta_m - \beta_n)}\int_{-\infty}^{\infty} \boldsymbol{E}_m^* \cdot \frac{\partial}{\partial z}\epsilon \cdot \boldsymbol{E}_n\, dx \tag{7}$$

where $\boldsymbol{E}_m$ and $\boldsymbol{E}_n$ are electric field vectors of the TM modes, P is the power carried by the mode, ω is the

radian frequency, and the asterisk indicates the complex conjugate. The coupled modes in (7) may be either guided modes or radiation modes. Following the mathematical procedures in [13, pp. 116–121] under the condition that the slopes of the tapered and separating sections are very gradual, we obtain

$$C_{mn} = \frac{\omega \tan\theta_t}{4P(\beta_m - \beta_n)} \left\{ \left[F(E_{px}, E_{qz}) \right]_{x=f(z)} + \left[F(E_{px}, E_{qz}) \right]_{x=-f(z)} \right\} \quad (8)$$

in the tapered section and

$$C_{mn} = \frac{\omega \tan\theta_b}{4P(\beta_m - \beta_n)} \cdot \left\{ \left[F(E_{px}, E_{qz}) \right]_{x=f(z)} + \left[F(E_{px}, E_{qz}) \right]_{x=-f(z)} - \left[F(E_{px}, E_{qz}) \right]_{x=h(z)} - \left[F(E_{px}, E_{qz}) \right]_{x=-h(z)} \right\} \quad (9)$$

in the separating section, where

$$F(E_{px}, E_{qz}) = \left[\frac{\epsilon_{rxx}}{\epsilon_{dxx}} (\epsilon_{rxx} - \epsilon_{dxx}) E_{mx}^* E_{nx} + (\epsilon_{rzz} - \epsilon_{dzz}) E_{mz}^* E_{nz} + \epsilon_{rxz} \log \frac{\epsilon_{rxz}}{\epsilon_{dxz}} (E_{mx}^* E_{nz} + E_{mz}^* E_{nx}) \right]. \quad (10)$$

In the above equations, θ_t and θ_b are the slopes of the tapered and separating sections, respectively, and E_{px} and E_{qz} are the x and z components of $\boldsymbol{E}_p$ and $\boldsymbol{E}_q$, where $p = m$ or n and $q = m$ or n. The field components should be evaluated right at the core boundaries inside the core. Readers can refer to [11] for functional expressions of guided modes in a three-layered slab waveguide. Those of the other modes will not be given here because the derivation for them, while quite straightforward, is uninteresting.

III. Practical Designs for Low-Loss Optical Branching Waveguides

Two practical structures have been proposed to reduce mode-conversion losses for branching waveguides composed of isotropic materials [5]–[7]. Here we apply these design considerations to those composed of anisotropic materials, and estimate mode-conversion losses in the branching waveguides. The coupled mode equations, (3) and (4), are solved by means of the Runge–Kutta–Gill method where the continuum of radiation modes with real propagation constants is divided uniformly into 120 discrete modes in the ρ space and the step length in the z direction is assumed to be $\Delta z = 0.25d$ in the actual computations.

A. Theory of Mode Transducer [5]

First let us summarize the theory of the mode transducer for two-mode transmission systems. We consider the cascade junction of two coupling regions A and B with

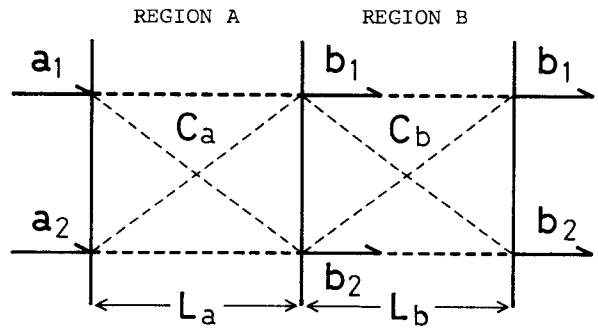

Fig. 3. Cascade junction of coupling regions. With an optimal design of A and B, an incident mode is converted to a designated normal mode in B through the propagation in A.

different types of local normal modes as illustrated in Fig. 3. Both input and output waveguides support two modes without any coupling between them. The normal modes in region B are assumed to be the same as those in the output waveguide. It is also assumed that reflected waves are negligible at any place. The coupled-mode equation in region A is given by

$$\frac{d}{dz} \begin{pmatrix} a_1(z) \\ a_2(z) \end{pmatrix} = j \begin{pmatrix} \beta_{a1} & C_a \\ C_a^* & \beta_{a2} \end{pmatrix} \begin{pmatrix} a_1(z) \\ a_2(z) \end{pmatrix} \quad (11)$$

where $a_m(z)$ and β_{am} are the amplitude coefficient and propagation constant of the normal mode labeled m, and C_a is the coupling coefficient. With the incident condition $[a_1(0), a_2(0)]$ at $z = 0$, the solution of (11) at $z = L_1$ is obtained as

$$\begin{pmatrix} a_1(L_1) \\ a_2(L_1) \end{pmatrix} = \exp\{j\gamma_a L_1\} \begin{pmatrix} \Omega_{11} & \Omega_{12} \\ \Omega_{21} & \Omega_{22} \end{pmatrix} \begin{pmatrix} a_1(0) \\ a_2(0) \end{pmatrix} \quad (12)$$

where

$$\begin{aligned} \Omega_{11} &= \cos\Gamma_a L_1 + j\Delta_a \sin(\Gamma_a L_1)/\Gamma_a \\ \Omega_{12} &= \Omega_{21}^* = jC_a \sin(\Gamma_a L_1)/\Gamma_a \\ \Omega_{22} &= \cos\Gamma_a L_1 - j\Delta_a \sin(\Gamma_a L_1)/\Gamma_a \\ \gamma_a &= (\beta_{a1} + \beta_{a2})/2 \\ \Gamma_a &= \sqrt{\Delta_a^2 + |C_a|^2} \\ \Delta_a &= |\beta_{a1} - \beta_{a2}|/2. \end{aligned} \quad (13)$$

On the other hand, the kth normal mode in region B can be expressed as

$$\boldsymbol{b}_k(z) = \boldsymbol{e}_{bk} \exp\{j\alpha_{bk}(z - L_1)\} \quad (14)$$

with $k = 1$ or 2. Here $\boldsymbol{e}_{bk}$ and α_{bk} are the kth eigenvector and eigenvalue of the matrix

$$C_b = \begin{pmatrix} \beta_{b1} & C_b \\ C_b^* & \beta_{b2} \end{pmatrix} \quad (15)$$

where β_{bm} is the propagation constant of the normal mode labeled m, and C_b is the coupling coefficient. We concentrate our discussion on a problem of power transfer to the b_1 mode from the a_1 mode. The first eigenvalue of (15) is given by

$$\alpha_{b1} = \gamma_b + \Gamma_b \tag{16}$$

with

$$\gamma_b = (\beta_{b1} + \beta_{b2})/2$$
$$\Gamma_b = \sqrt{\Delta_b^2 + |C_b|^2}$$
$$\Delta_b = |\beta_{b1} - \beta_{b2}|/2 \tag{17}$$

and the associated eigenvector is expressed as

$$e_{b1} = [1, (\Gamma_b - \Delta_b)/C_b]. \tag{18}$$

For the complete transfer of power, we should require

$$\begin{pmatrix} b_1(L_1) \\ b_2(L_1) \end{pmatrix} = \begin{pmatrix} a_1(L_1) \\ a_2(L_1) \end{pmatrix} = a_1(L_1) \begin{pmatrix} 1 \\ (\Gamma_b - \Delta_b)/C_b \end{pmatrix}. \tag{19}$$

Substituting (12) and (13) into (19) with the incident condition $a_2(0) = 0$ and equating both real and imaginary parts of the resultant equation, we get

$$\zeta_a = \left(\sqrt{1+\zeta_b^2} - 1\right)/\zeta_b \tag{20}$$

$$L_a = (2N+1)\pi / \left(2\Delta_a \sqrt{1+\zeta_a^2}\right), \qquad N = 0, 1, 2, \cdots \tag{21}$$

where

$$\zeta_p = |C_p|/\Delta_p, \qquad p = a \text{ or } b. \tag{22}$$

Structural parameters in the coupling regions A and B can be determined by applying (20) and (21). In the case of $\zeta_a \ll 1$ and $\zeta_b \ll 1$ with $N = 0$, (20) and (21) reduce to

$$L_a \simeq \frac{\pi}{2\Delta_a} \tag{23}$$

$$\frac{\zeta_a}{\zeta_b} \simeq \frac{1}{2}. \tag{24}$$

B. Design Method I

Before we discuss low-loss branching waveguides, we analyze mode-conversion phenomena in oblique propagation in the conventional branching waveguide shown in Fig. 1. In the numerical calculations, it is assumed that $L_f = 78.645d$, that $\theta = 1°$, and that the waveguide is composed of $LiNbO_3$ with the refractive indices $\sqrt{\epsilon_{d1}/\epsilon_0} = 2.272$ and $\sqrt{\epsilon_{d3}/\epsilon_0} = 2.187$. The elements of the dielectric tensors in both the core and the cladding region satisfy the following relation:

$$\epsilon_{rij} = \epsilon_{dij}(1+\delta), \qquad i \text{ or } j = x, y, \text{ or } z \tag{25}$$

where $\delta = 0.0201$. In addition, we define the normalized frequency as

$$V = k_0 d \sqrt{\eta_r(\epsilon_{rxx} - \epsilon_{dxx})/\epsilon_0 \epsilon_{rxx}^2}. \tag{26}$$

With V chosen equal to π except for the tapered section, only the lowest-order guided TM_0 mode, the incident mode on the branching waveguide, can be supported. At the output end of the tapered section, the waveguide width is $2d$. This means that the guided TM_1 mode can be excited halfway in the tapered section. Consequently the guided TM_0 mode, guided TM_1, even TM radiation, and odd TM radiation modes exist in the structure as the coupled modes. Fig. 4 shows the change of power of the coupled modes as a function of oblique angle. The ordinates represent the coupled mode power:

$$P_{cm} = \begin{cases} P|a_n(L_f)|^2 & \text{for guided modes} \\ P\int_0^{\sqrt{\eta_d/\epsilon_0 \epsilon_{dxx}} k_0} |a_r(L_f, \rho)|^2 \, d\rho & \text{for radiation modes} \end{cases} \tag{27}$$

which is normalized by the power of the incident mode. It can be seen from Fig. 4 that mode conversion is strongest between the incident mode and the even TM radiation modes, and reaches its maximum value at $\alpha = 0°$. The characteristics of mode conversion to the odd modes, the guided TM_1 and odd TM radiation modes, are illustrated in Fig. 4(c). This type of coupling, which never occurs in the isotropic case, is caused by the nondiagonal elements of the dielectric tensor. The coupled power of the guided TM_1 mode caused by mode conversion reaches its peak at $\alpha = 45°$, where both ϵ_{pxz} and ϵ_{pzx} in (2) become maximum.

Taking these results into account, we concentrate our discussion in the following on the case of $\alpha = 0°$, where mode-conversion losses are most significant. The first low-loss branching waveguide (structure I) is designed as shown in Fig. 5. This is made up of four subsections: a tapered section of slope θ_t succeeding a single slab waveguide; a prong waveguide of slope θ_{b1} as the first mode converter; a main separating section of slope θ_{b2}; and a second mode converter composed of two slab waveguides of slope θ_{b3}. Two parallel slab waveguides with a separation of h follow the last subsection. The width of waveguide is assumed to be d everywhere except for the tapered section. L_t, L_{b1}, and L_{b3} are the lengths of subsections I, II, and IV, respectively, and L_f is the overall length of the branching waveguide. Subsections II and IV correspond to coupling region A in Fig. 3, and subsection III corresponds to coupling region B. The tapered section, subsection I, has a constant slope in the present paper because the radiation losses at the tapered section are much less than those in a prong waveguide. We apply the above-mentioned theory here to the guided TM_0 mode and the radiation mode having the largest coupling coefficient. Considering that the coupling coefficients are almost proportional to the slope of the wave-

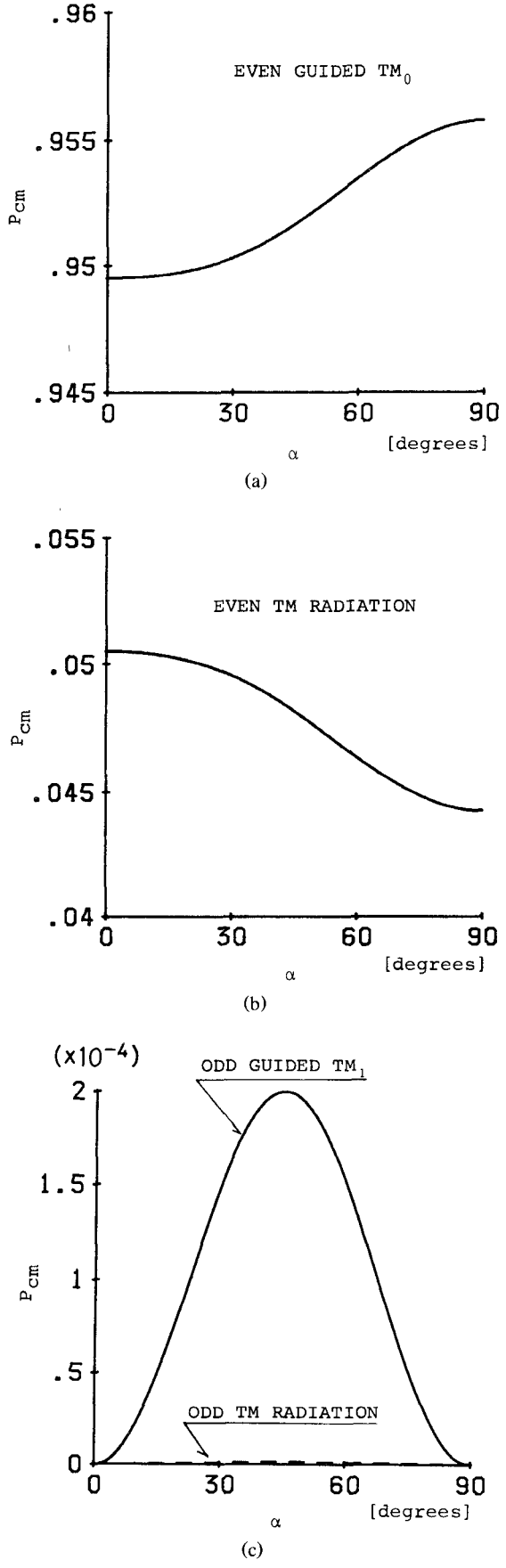

Fig. 4. Variation in the coupled-mode power caused by mode conversion in the conventional branching waveguide as a function of oblique angle, where $\theta = 1°$ and $L_f = 78.645d$.

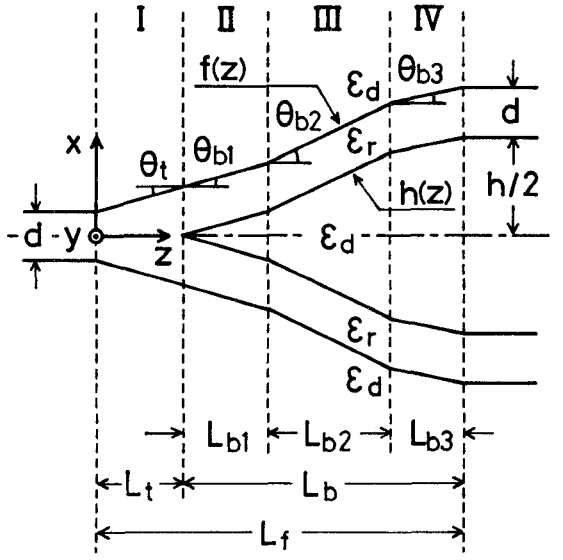

Fig. 5. Branching waveguide of structure I.

guide, the parameters of the structure in Fig. 5 are determined to be [6], [7]

$$L_{b1} = \frac{\pi}{\beta_0(L_t) - \beta_r(L_t, \rho)}$$

$$L_{b3} = \frac{\pi}{\beta_0(L_f) - \beta_r(L_f, \rho)}$$

$$L_t = \frac{d}{d+h} L_f - \frac{L_{b1} + L_{b3}}{2}$$

$$\theta_t = \theta_{b1} = \theta_{b3} = \theta_{b2}/2. \tag{28}$$

In the above equations, $\beta_0(L_t)$ and $\beta_0(L_f)$ are the propagation constants of the guided TM_0 mode at $z = L_t$ and L_f, and $\beta_r(L_t, \rho)$ and $\beta_r(L_f, \rho)$ are the constants of the even TM radiation mode having the maximum coupling coefficient with the former guided mode at $z = L_t$ and L_f, respectively.

Power losses caused by mode conversion to the radiation modes are illustrated in Fig. 6, where the abscissas are the total length L_f of the branching waveguide and the ordinates the normalized power of the radiation modes. The solid lines indicate the radiation losses in structure I. The dotted lines indicate those in the conventional branching waveguide which has the same length and the same branch separation as structure I. The slope of the conventional branching waveguide is given by

$$\theta = \tan^{-1}\left(\frac{h+d}{2L_f}\right). \tag{29}$$

The half span of the branch separation is assumed as $h/2 = 0.625d$ in Fig. 6(a) and $h/2 = 1.25d$ in Fig. 6(b). It is found from the figure that, in most regions of L_f, the characteristics of the mode-conversion losses in structure I are superior to those in the conventional branching waveguide. It is expected that the mode-conversion losses can be drastically reduced by utilizing the branching waveguide proposed here.

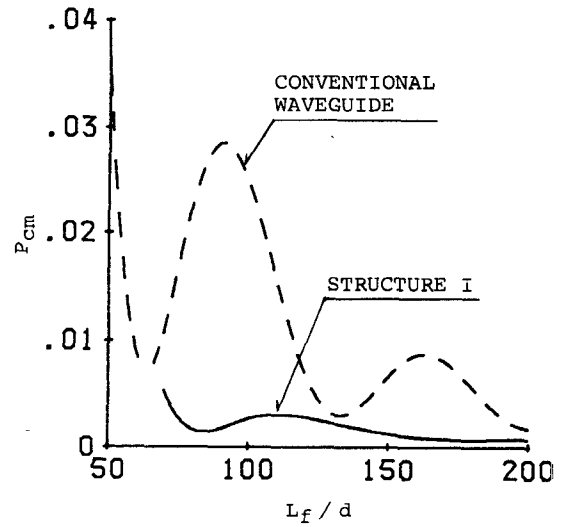

(a)

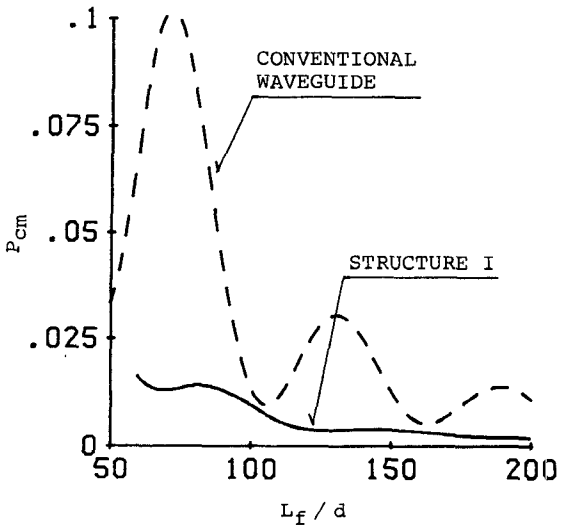

(b)

Fig. 6. Variation in the radiation losses in the branching waveguides shown in Figs. 1 and 5 as a function of the total length L_f of the structure, where (a) $h/2 = 0.625d$ and (b) $h/2 = 1.25d$.

C. Design Method II

The second branching waveguide (structure II) is shown in Fig. 7. The whole structure is made up of three subsections, that is, a tapered section of slope θ_1 succeeding a single slab waveguide; a separating section of slope θ_2; and two slab waveguides of slope θ_3 followed by two parallel slab waveguides with a separation of h. L_1, L_2, and L_3 are the lengths of subsections I, II, and III, respectively. In this case, subsections I and III correspond to regions A and B in Fig. 3, respectively. By means of (23) and (24) the above parameters are determined to be

$$L_1 = \frac{\pi}{\beta_0(0) - \beta_r(0,\rho)}$$

$$L_3 = \frac{\pi}{\beta_0(L_f) - \beta_r(L_f,\rho)}$$

$$\theta_1 = \tan^{-1}\left(\frac{d}{2L_1}\right) \tag{30}$$

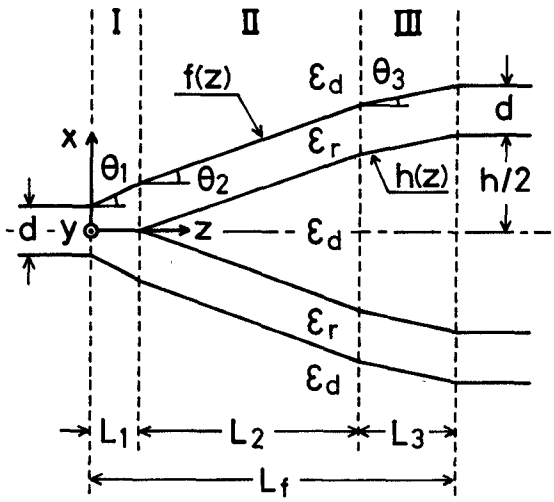

Fig. 7. Branching waveguide of structure II.

where $\beta_0(0)$ and $\beta_0(L_f)$ are the propagation constants of the guided TM_0 mode at $z = 0$ and L_f, and $\beta_r(0,\rho)$ and $\beta_r(L_f,\rho)$ are the constants of the even TM radiation mode having the maximum coupling coefficient with the former guided mode at $z = 0$ and L_f, respectively. Since the coupling coefficients between the guided TM_0 mode and the even TM radiation modes are in proportion to the slope of the waveguide, we define the following relation between the slopes as [6]

$$\theta_3 = \theta_2/2 = \theta_1/2M \tag{31}$$

where the parameter M is a positive constant called the angle ratio that is introduced to optimize the mode transducer. According to the numerical calculation, the coupling coefficient in the separating section is about four times as large as that in the tapered section with the same slope. We can easily guess from this fact that the optimum condition will be obtained at $M = 2$ or so. The length L_2 of subsection II can be determined as

$$L_2 = \frac{h/2 - L_3 \tan\theta_3}{\tan\theta_2}. \tag{32}$$

In the numerical calculations, all of the structural and material parameters are assumed to be the same as those in structure I. Mode-conversion losses to the radiation modes are illustrated in Fig. 8, where the abscissas are the total length L_f or the angle ratio M, and the ordinates the normalized power of the radiation modes. The solid lines indicate the radiation losses in structure II. The dotted lines indicate those in the conventional branching waveguide which has the same length and the same branch separation as structure II. Therefore, the slope of the conventional branching waveguide is given by

$$\theta = \tan^{-1}\left\{\frac{h+d}{2(L_1+L_2+L_3)}\right\}. \tag{33}$$

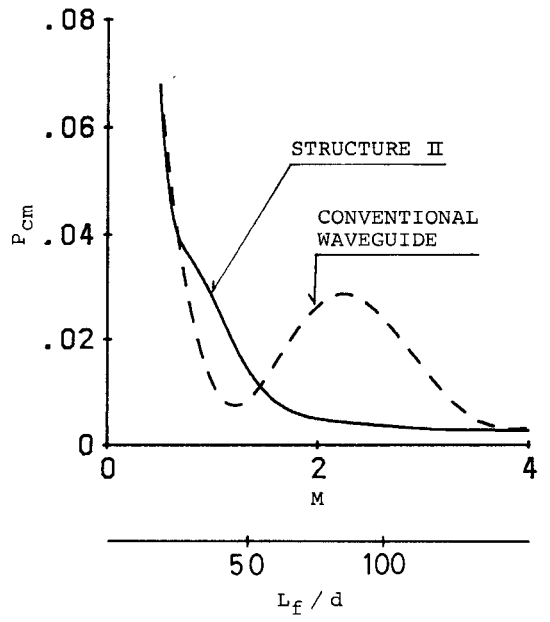

(a)

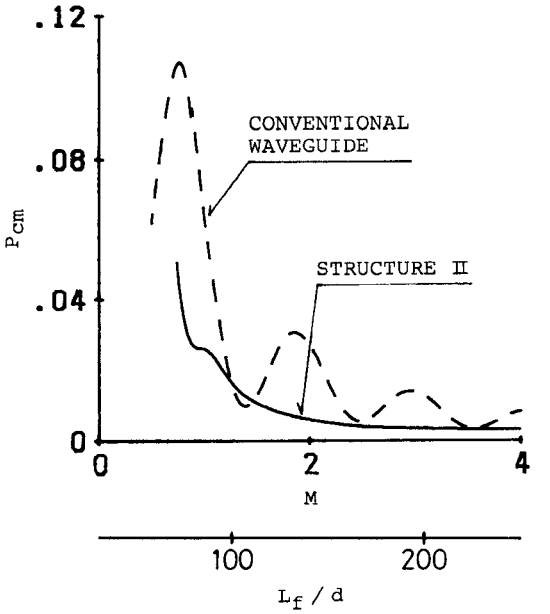

(b)

Fig. 8. Variation in the radiation losses in the branching waveguides shown in Figs. 1 and 7 as a function of the angle ratio M or total length L_f of the structure, where (a) $h/2 = 0.625d$ and (b) $h/2 = 1.25d$.

The half span of the branch separation is $h/2 = 0.625d$ in Fig. 8(a) and $h/2 = 1.25d$ in Fig. 8(b). As a result, a significant reduction of the radiation losses can be expected when the angle ratio M is larger than 2.5.

Fig. 9 shows the mode-conversion losses for the case of $M = 2.5$ as a function of the half span of the branch separation. The solid line indicates the radiation losses in structure II, and the dotted line indicates those in the conventional branching waveguide. It is found that the radiation losses in the conventional structure are much larger than those in the proposed branching waveguide over the entire region of the abscissa shown in the figure.

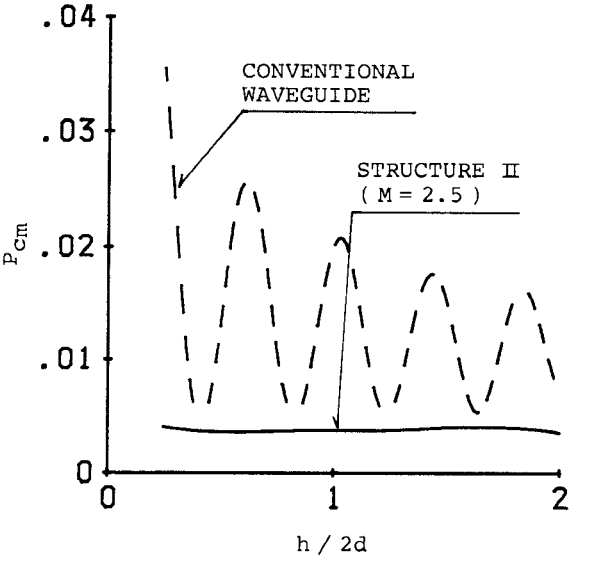

Fig. 9. Mode-conversion losses in the branching waveguides shown in Figs. 1 and 7 as a function of the half span of the branching separation, where $M = 2.5$ in structure II.

IV. Conclusions

Two low-loss branching waveguides consisting of anisotropic materials are proposed and the characteristics of mode conversion in these waveguides are numerically analyzed by means of coupled-mode theory. The branching waveguides proposed here have two mode-conversion sections on both input and output sides of conventional symmetric branching waveguides. The analysis is devoted to the TM mode since it exhibits interesting behavior owing to mode conversion in oblique propagation which cannot be observed in waveguides composed of isotropic materials. Numerical results show that the branching waveguides proposed in this paper incur much lower mode-conversion losses than conventional branching waveguides.

Acknowledgment

The authors wish to thank their colleague Dr. Kazuo Ono, Department of Electronics Engineering, Ehime University, for many helpful discussions.

References

[1] H. Yajima, "Coupled mode analysis of dielectric planar branching waveguides," *IEEE J. Quantum Electron.*, vol. QE-14, pp. 749–755, Oct. 1978.

[2] H. Yajima, "Coupled-mode analysis of anisotropic dielectric planar branching waveguides," *J. Lightwave Technol.*, vol. LT-1, pp. 273–279, Mar. 1983.

[3] T. R. Ranganath and S. Wang, "Ti-diffused $LiNbO_3$ branched-waveguide modulators: Performance and design," *IEEE J. Quantum Electron.*, vol. QE-13, pp. 290–295, Apr. 1977.

[4] R. C. Alferness, "Guided-wave devices for optical communication," *IEEE J. Quantum Electron.*, vol. QE-17, pp. 946–959, June 1981.

[5] S. Sawa, "A design theory of mode transducers utilizing coupling effects of multi-mode coupling system and its applications," *Trans. IEICE(Japan)*, vol. J70-C, pp. 858–867, June 1987.

[6] S. Sawa, K. Ono, and S. Mori, "Design considerations for mode-conversion type optical branching waveguide," *Trans. IEICE (Japan)*, vol. J71-C, pp. 432–443, Mar. 1988.

[7] S. Sawa, K. Ono, and S. Mori, "Design method multi-mode Y branch waveguides," *Trans. IEICE(Japan)*, vol. J72-C-I, pp. 568–570, Sept. 1989.
[8] O. Hanaizumi, M. Miyagi, and S. Kawakami, "Low radiation loss Y-junctions in planar dielectric optical waveguides," *Optics Commun.*, vol. 51, pp. 236–238, Sept. 1984.
[9] L. M. Johnson and F. J. Leonbergber, "Low-loss $LiNbO_3$ waveguide bends with coherent coupling," *Optics Lett.*, vol. 8, pp. 111–113, Feb. 1983.
[10] R. A. Becker and L. M. Johnson, "Low-loss multiple-branching circuit in Ti-indiffused $LiNbO_3$ channel waveguides," *Optics Lett.*, vol. 9, pp. 246–248, June 1984.
[11] D. Marcuse, "Modes of a symmetric slab optical waveguide in birefringent media—Part I: Optical axis not in plane of slab," *IEEE J. Quantum Electron.*, vol. QE-14, pp. 736–741, Oct. 1978.
[12] D. Marcuse and I. P. Kaminow, "Modes of a symmetric slab optical waveguide in birefringent media, Part II: Slab with coplanar optical axis," *IEEE J. Quantum Electron.*, vol. QE-15, pp. 92–101, Feb. 1979.
[13] D. Marcuse, *Theory of Dielectric Optical Waveguides*. New York: Academic Press, 1974.

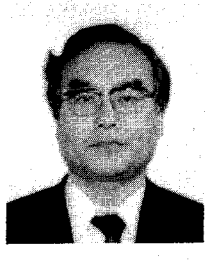

Shinnosuke Sawa (M'72) was born in Osaka, Japan, on October 23, 1938. He received the B.E. degree in electrical engineering from the University of Osaka Prefecture, Osaka, Japan, in 1962, and the M.E. and Ph.D. degrees, both in electrical communication engineering, from Osaka University, Osaka, Japan, in 1967 and 1970, respectively.

From 1962 to 1964 he worked in industry for the Mitsubishi Electric Corporation, where he was engaged in ignitron manufacturing and vacuum switch development at the Kyoto plant. From 1970 to 1976 he was an Associate Professor in the Department of Electronics at Ehime University, Matsuyama City, Japan, and from 1976 to January 1991 he was a Professor there. He is currently a Professor in the Electrical Engineering Department at the University of Osaka Prefecture, Sakai City, Osaka, Japan. He has been engaged in research and education on electromagnetic theory, microwave and millimeter-wave theory and applications, optical transmission lines, optical integrated circuits, and optoelectronics.

Dr. Sawa is a member of the Institute of Electronics, Information, and Communication Engineers of Japan, the Institute of Electrical Engineers of Japan, and the Laser Society of Japan.

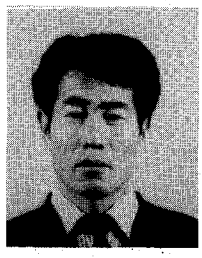

Masahiro Geshiro (S'75–M'78) received the B.E., M.E., and Ph.D. degrees in 1973, 1975, and 1978, respectively, from Osaka University, Osaka, Japan.

In December 1979 he joined the Department of Electronics, Ehime University, Matsuyama, Japan, where he is now an Associate Professor of Electronics Engineering. From March 1986 to January 1987, he was a Visiting Scholar at the University of Texas at Austin, on leave from Ehime University. He has been engaged in research on microwave and optical-wave transmission lines and integrated optics.

Dr. Geshiro is a member of the Institute of Electronics, Information, and Communication Engineers of Japan.

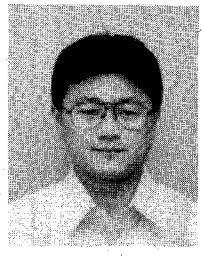

Fumikazu Takeda was born in Ehime, Japan, on March 6, 1966. He received the B.E. and M.E. degrees in electronics engineering from Ehime University, Ehime, Japan, in 1988 and 1990, respectively. Since 1990 he has been with RNB, Nankai Broadcasting Company, Ehime, Japan.

Mr. Takeda is a member of the Institute of Television Engineers of Japan.